

## 9.3. X-RAY DIFFRACTION IMAGING OF WHOLE CELLS

chromosome because of morphological changes which occurred during data collection. Hence, full three-dimensional imaging of cells by diffractive methods requires cryogenic protection against radiation damage. Predictions based on a calculation of the cross section for coherent scattering by a smooth dielectric indicate that 10 nm resolution imaging of frozen hydrated organic matter should be possible using soft X-rays at currently available synchrotron sources (Howells *et al.*, 2009). This limit is arrived at through a comparison of the radiation dose required for imaging and the dose at which radiation damage has been empirically observed at different length scales. However, it seems plausible that the presence of many identical particles within a cell could be exploited to provide super-resolution information.

## 9.3.3.2. Low-dose three-dimensional imaging; low damage potential of stereoscopic viewing

Diffraction imaging in three dimensions proceeds as it does in standard X-ray tomography. That is, two-dimensional data are recorded from many angular orientations of the sample and then assembled into a three-dimensional data set. In this case, however, the data are recorded in reciprocal space and the individual data sets only need to be registered with respect to the angular coordinate due to the Fourier shift theorem. In the absence of any additional information, the angular sampling of

reciprocal space is determined by the Crowther resolution,

$$k_C = \frac{1}{\Delta\theta D},$$

where  $D$  is the object diameter and  $\Delta\theta$  is the angular separation of the two-dimensional data sets. This is the spatial frequency at which the unmeasured Fourier components, those in between the measured Ewald sphere segments, can be properly interpolated from the measured data. Diffraction microscopy, however, requires the addition of information in the form of real-space constraints. This additional information allows for the calculation of not only the missing reciprocal-space phases but also a limited number of missing magnitudes. Chapman *et al.* (2006) showed that  $\Delta\theta$  could in fact be up to four times larger than required by the Crowther relation, with  $k_C$  matching the numerical aperture of the imaging system. Thus, three-dimensional reconstructions could take place with nearly isotropic diffraction-limited resolution with only about 150 angular orientations of the sample.

Stereoscopic viewing can provide a significant degree of three-dimensional perception of an extended object while only increasing the total radiation exposure by a factor of two. In principle, according to the dose-fractionation theorem of Hegerl and Hoppe, full three-dimensional visualization of a given resolution element should not require a dose any higher than two-dimensional visualization of the same element with the same statistical accuracy (Hegerl & Hoppe, 1976). This theorem provides hope that high-resolution imaging in three-dimensions, perhaps even of dry specimens, is possible, but in practice this is very difficult to achieve and low-dose imaging techniques are only now being explored by the CXDM community. Stereoscopic viewing should be considered the preliminary low-dose technique of choice. One particular advantage is the rapid reconstruction (compared with full three-dimensional reconstructions) which makes possible *in situ* sample inspection. Fig. 9.3.3.2 shows a stereo image of a chemically dried budding yeast cell. When viewed stereoscopically, with the viewer's focus in front of the image, the three-dimensional arrangement of a group of vesicles in the mother cell can be visualized.

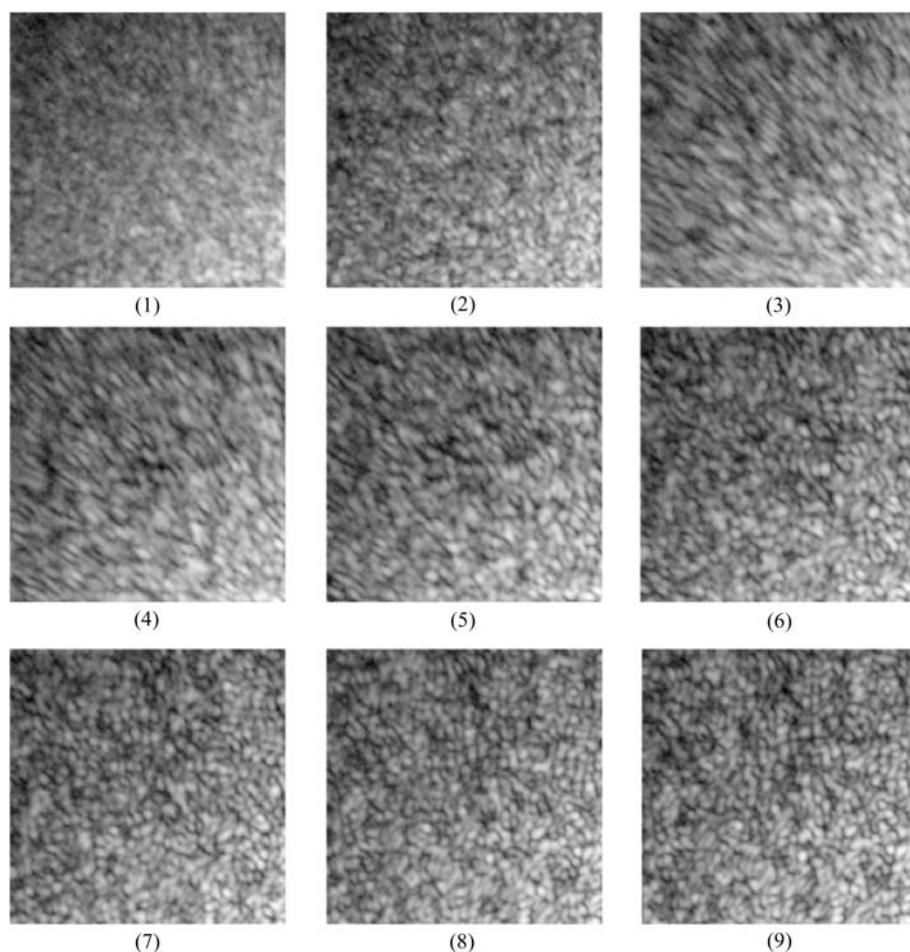


**Figure 9.3.3.2**

Exposure to ionizing radiation causes shrinkage of organic matter. Each image in this series is a section of a measured diffraction pattern from a freeze-dried yeast cell. The images were taken sequentially and each represents an additional X-ray dose of  $5 \times 10^8$  Gy. After a cumulative dose of  $1 \times 10^9$  Gy, the cell undergoes a rapid collapse [apparent from the elongated speckles in images (3)–(5)] followed by continued shrinkage at a reduced rate. The X-rays used had an energy of 750 eV and a dose of  $5 \times 10^8$  Gy was adequate for reconstruction at 30 nm resolution. (Reproduced from Shapiro, 2004).

## 9.3.4. Conclusions

CXDM promises to be a highly efficient imaging methodology which can deliver high-resolution and high-contrast images of large non-crystalline biological structures. Radiation-induced shrinkage of dry cells will probably prohibit three-dimensional imaging of such cells at high resolution. However, significant three-dimensionality can be achieved through stereoscopic viewing of a cell, which only doubles the necessary X-ray dose. Even so, in the absence of low-dose diffraction techniques the sample must undergo considerable morphological change prior

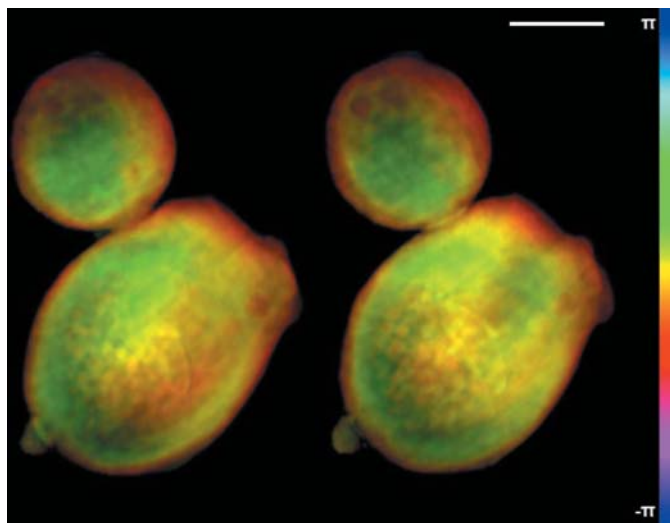


**Figure 9.3.3.3**

Stereo image of a budding yeast cell. This budding yeast cell was chemically fixed with glutaraldehyde and dehydrated in acetone. The images have an angular separation of  $10^\circ$  and a pixel size of 11 nm. The three-dimensional arrangement of a group of small vesicles in the mother cell can be visualized when viewed stereoscopically (with the viewer's focus in front of the image). The scale bar is 500 nm.

to imaging, although this change does not seem to alter the relative arrangement of organelles. The development of low-dose techniques will allow for the direct observation of these radiation-induced changes. In the long run, it is cryogenic protection that provides the most valuable structural information, since the cells are maintained in a near living state. Ultra-high-resolution three-dimensional imaging will still require the development of low-dose techniques, as cryoprotected samples have also been observed to suffer from mass loss with the accumulation of very high X-ray doses ( $>10^{10}$  Gy). These imaging techniques are currently under development at the ALS in collaboration with Stony Brook University and elsewhere. Alternatively, X-ray free-electron lasers (FELs) promise the highest resolution imaging of living cells that is possible by any means; indeed, it has been proposed that sub-nanometre resolution is possible (Bergh *et al.*, 2008). The ultra-short and ultra-bright pulses of an X-ray FEL will encode the structural information from a living cell before it is destroyed by the pulse.

The author would like to thank Johanna Nelson and Xiaojing Huang of Stony Brook University for preparing the samples and providing the diffraction data for reconstruction. This work was supported under the Seaborg Fellowship at Lawrence Berkeley National Laboratory and by grants from the National Institutes of Health, the National Science Foundation and the US Department of Energy to Stony Brook University. The Advanced Light Source at Lawrence Berkeley National Laboratory is supported by the Director, Office of Science, Office of Basic Energy Sciences, Materials Sciences Division, of the US Department of Energy.

### References

Barty, A., Marchesini, S., Chapman, H. N., Cui, C., Howells, M. R., Shapiro, D. A., Minor, A. M., Spence, J. C., Weierstall, U., Ilavsky, J., Noy, A., Hau-Riege, S. P., Artyukhin, A. B., Baumann, T., Willey, T., Stolken, J., van Buuren, T. & Kinney, J. H. (2008). *Three-dimensional coherent X-ray diffraction imaging of a ceramic nanofoam: determina-*

*tion of structural deformation mechanisms. Phys. Rev. Lett.* **101**, 055501.

Bates, R. H. T. (1982). *Fourier phase problems are uniquely soluble in more than one dimension. I. Underlying theory. Optik (Stuttgart)*, **61**, 247–262.

Bates, R. H. T. & Fright, W. R. (1983). *Composite two-dimensional phase-restoration procedure. J. Opt. Soc. Am.* **73**, 358–365.

Bergh, M., Huldt, G., Timneanu, N., Maia, F. R. & Hajdu, J. (2008). *Feasibility of imaging living cells at subnanometer resolutions by ultrafast X-ray diffraction. Q. Rev. Biophys.* **41**, 181–204.

Chao, W., Kim, J., Rekawa, S., Fischer, P. & Anderson, E. H. (2009). *Demonstration of 12 nm resolution Fresnel zone plate lens based soft X-ray microscopy. Opt. Express*, **17**, 17669–17677.

Chapman, H. N., Barty, A., Marchesini, S., Noy, A., Hau-Riege, S. P., Cui, C., Howells, M. R., Rosen, R., He, H., Spence, J. C., Weierstall, U., Beetz, T., Jacobsen, C. & Shapiro, D. (2006). *High-resolution ab initio three-dimensional X-ray diffraction microscopy. J. Opt. Soc. Am. A Opt. Image Sci. Vis.* **23**, 1179–1200.

Fienup, J. R. (1978). *Reconstruction of an object from the modulus of its Fourier transform. Opt. Lett.* **3**, 27–29.

Fienup, J. R. (1982). *Phase retrieval algorithms: a comparison. Appl. Opt.* **21**, 2758–2769.

Fienup, J. R. (1987). *Reconstruction of a complex-valued object from the modulus of its Fourier transform using a support constraint. J. Opt. Soc. Am. A Opt. Image Sci. Vis.* **4**, 118–123.

Fienup, J. R., Crimmins, T. R. & Holsztynski, W. (1982). *Reconstruction of the support of an object from the support of its autocorrelation. J. Opt. Soc. Am.* **72**, 610–624.

Gerchberg, R. W. & Saxton, W. O. (1972). *A practical algorithm for the determination of phase from image and diffraction plane pictures. Optik (Stuttgart)*, **35**, 237–246.

Hegerl, R. & Hoppe, W. (1976). *Influence of electron noise on three-dimensional image reconstruction. Z. Naturforsch. Teil A*, **31**, 1717–1721.

Howells, M. R., Beetz, T., Chapman, H. N., Cui, C., Holton, J. M., Jacobsen, C. J., Kirz, J., Lima, E., Marchesini, S., Miao, H., Sayre, D., Shapiro, D. A., Spence, J. C. H. & Starodub, D. (2009). *An assessment of the resolution limitation due to radiation damage in X-ray diffraction microscopy. J. Electron Spectrosc. Relat. Phenom.* **170**, 4–12.

Huang, X., Nelson, J., Kirz, J., Lima, E., Marchesini, S., Miao, H., Nieman, A. M., Shapiro, D., Steinbrener, J., Stewart, A., Turner, J. J. & Jacobsen, C. (2009). *Soft X-ray diffraction microscopy of a frozen hydrated yeast cell. Phys. Rev. Lett.* **103**, 198101.

Jearanaikoon, S. & Abraham-Peskir, J. V. (2005). *An X-ray microscopy perspective on the effect of glutaraldehyde fixation on cells. J. Microsc.* **218**, 185–192.

Larabell, C. A. & Le Gros, M. A. (2004). *X-ray tomography generates 3-d reconstructions of the yeast, *Saccharomyces cerevisiae*, at 60 nm resolution. Mol. Biol. Cell*, **15**, 957–962.

Le Gros, M. A., McDermott, G., Uchida, M., Knoechel, C. G. & Larabell, C. A. (2009). *High-aperture cryogenic light microscopy. J. Microsc.* **235**, 1–8.

Lima, E., Wiegart, L., Pernot, P., Howells, M. R., Timmins, J., Zontone, F. & Madsen, A. (2009). *Cryogenic X-ray diffraction microscopy for biological samples. Phys. Rev. Lett.* **103**, 198102.

Marchesini, S. (2007). *A unified evaluation of iterative projection algorithms for phase retrieval. Rev. Sci. Instrum.* **78**, 011301.

Marchesini, S., He, H., Chapman, H. N., Hau-Riege, S. P., Noy, A., Howells, M. R., Weierstall, U. & Spence, J. C. H. (2003). *X-ray image reconstruction from a diffraction pattern alone. Phys. Rev. B*, **68**, 140101.

Miao, J., Charalambous, P., Kirz, J. & Sayre, D. (1999). *Extending the methodology of X-ray crystallography to allow imaging of micrometre-sized non-crystalline specimens. Nature (London)*, **400**, 342–344.

Miao, J., Ishikawa, T., Johnson, B., Anderson, E. H., Lai, B. & Hodgson, K. O. (2002). *High resolution 3D X-ray diffraction microscopy. Phys. Rev. Lett.* **89**, 088303.

Miao, J., Sayre, D. & Chapman, H. N. (1998). *Phase retrieval from the magnitude of the Fourier transforms of nonperiodic objects. J. Opt. Soc. Am. A Opt. Image Sci. Vis.* **15**, 1662–1669.

Nelson, J., Huang, X., Steinbrener, J., Shapiro, D. A., Kirz, J., Marchesini, S., Neiman, A. M., Turner, J. & Jacobsen, C. (2010). *High resolution X-ray diffraction microscopy of specifically labelled yeast cells. Proc. Natl. Acad. Sci. USA*, **107**, 7235–7239.